

Optimization of DC and AC performances for Al_{0.26}Ga_{0.74}N/GaN/4H-SiC HEMT with 30nm T-gate

Imane Four^{1*} and Mohammed Kameche²

¹ STIC Laboratory, Abou-bekr Belkaid University of Tlemcen, Algeria.

² The Satellite Development Centre Oran, Algeria.

Received 1 January 2020, Revised 24 February 2020, Accepted 6 April 2020

ABSTRACT

The main purpose of this paper is to inquire about the DC and AC performances of AlGa_N/Ga_N high electron mobility transistors structure based on innovational II-N materials with 4H-SiC substrate and 30 nm gate length. First, the structure was designed with optimized physical and geometric parameters. Second, DC and AC performance have been studied. The device exhibits a maximum drain current of 600 mA/mm, a threshold voltage of -3.5 V, a maximum transconductance of 200 mS /mm, an Ion/Ioff ratio of 109, DIBL of 22 mV/V, and SS of 200 mV/dec. Furthermore, remarkable AC performance in terms of cut-off frequency (F_t) and maximum oscillation frequency (F_{max}) has been attained. This outstanding DC and AC performances make them a splendid candidate for future high power and high frequency application.

Keywords: HEMT, AlGa_N/Ga_N, DC Performance, AC Performance.

1. INTRODUCTION

Over recent years, gallium nitride (GaN) technologies, with a direct bandgap energy of 3.49 eV, have outstanding intrinsic qualities such as high thermal conductivity, high breakdown, and high electron mobility. These technologies are therefore a promising area for the development of systems that require high levels of power in the microwave domain: space, defence, and automotive. Meanwhile, the ample growth of communication systems demands to increase the power delivering capability in the microwave frequency range, where GaAs or InP devices had been performing major roles. Such situation steered the development of GaN-based microwave power devices, which proved high output power with high gain in extremely small chip size [1].

Gallium Nitride (GaN) high electron mobility transistors (HEMTs) have recently been able to take part in silicon-based transistors (Si) and gallium arsenide (GaAs)-based pHEMT's market for base stations used for telecommunications. Wide bandgap semiconductors and particularly III-V compounds, as GaN and its alloys, by their physical and chemical properties are a good contender for the implementation of such components characterized by high power at high frequency [2]. In fact, their crystallographic structures give out properties such as high thermal conductivity, a strong breakdown field and, high saturation speeds that are essential for satellite applications [3]. The feature of this kind of structure is to create a two-dimensional electron gas (2DEG) through a heterojunction. It is selected to create a localized potential fall of the conduction band under the Fermi level and confining carriers in a good quantum well. The potential barrier thus created, and the corresponding diagrams are functions of the forbidden bands of each of the semiconductors used and the respective doping. The electron exchange that

*Corresponding Author: imane.four@student.univ-tlemcen.dz

takes place between the two semiconductors at the junction, allows the aligning of the Fermi levels [4].

The performance of AlGa_N/Ga_N HEMT can be affected by the phenomena of traps which come from impurities located in the semiconductor that will capture and re-emit charge carriers. Therefore, it does not participate in the electron conduction and the drain current of the transistor is reduced as reported in the previous work [5].

Another possible constraint is self-heating. It is due to a strong current flowing in an extended way in the two-dimensional channel creates thermal effects due to the increase of the collisions between the free electrons and the crystal lattice. Therefore, the mobility of the electrons decreases consequently, and it results in a decline of the drain current [2]. It induces a reduction of the transconductance and the power output in RF. Besides, to improve device performance, several optimization methods were carried out.

As was proved in the work [5], using Si₃N₄ as passivation layer exhibit remarkable increase in drain current densities with a compromise of increased gate leakage, as well minimizing the trapping effects which influence the performance of HEMT. In addition, the work [7] shows that the back-barrier layer is efficient to ensure a drain induced barrier lowering (DIBL) and keeping the reduction of subthreshold swing (SS) caused by channel effects. As was pointed in [2], using 4H-SiC as substrate which has a high thermal conductivity able to maintain a good heat transfer and prevent self-heating.

This paper studies the DC and AC performances of HEMT based on AlGa_N/Ga_N/4H-SiC with Si₃N₄ passivation layer and T shape gate. The importance of III-V materials for high frequency and high-power applications was also demonstrated.

This paper is organized into the following parts: the first section introduces the simulation of passivated and non-passivated HEMT structure, and the comparison of the obtained results. A second section is dedicated to the presentation of the proposed structure that used different physical and geometrical parameters. The third section contains the simulated DC and AC characteristics. Moreover, a comparison of our result was realized. Finally, a general conclusion is presented.

2. COMPARISON OF PASSIVATED AND NON-PASSIVATED STRUCTURE

Recently, the work done in [6] was based on AlGa_N/Ga_N HEMT. Their structure yields a negative conductance at large V_d because of the self-heating. On the other side, traps effect appeared on the surface of the HEMT which can reduce the performance of the device. Therefore, it is important to deposit a passivation layer to avoid all this issue and improve the performance of the device. First, the structure of [6] was simulated with and without the passivation layer. After that, the result was compared.

Figure 1(a) describes the structure which consists of 500 nm of AlN/AlGa_N buffer, 1.8 μm Ga_N channel, 23 nm thick of Al_{0.26}Ga_{0.74}N barrier and 1 nm n⁺-Ga_N cap layer. The gate has a length of 0.25 μm. The distance of gate-source and the gate-drain are 0.77 μm and 1.32 μm, respectively [6]. Figure 1(b) shows the same dimension with the additional passivation layer of Si₃N₄ by using SILVACO TCAD simulator.

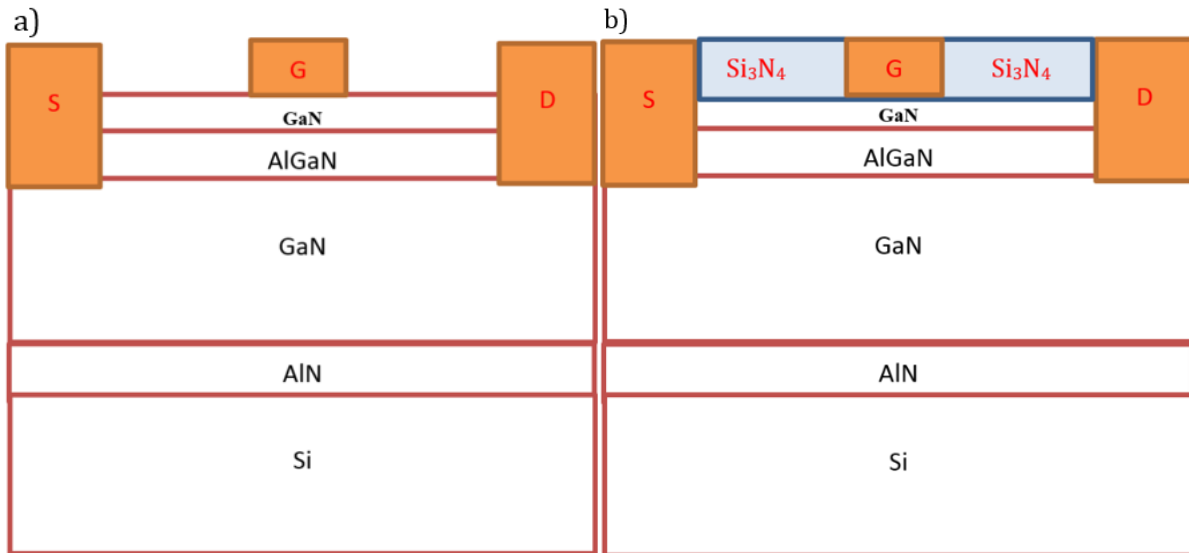


Figure 1. The structure of AlGaN/GaN HEMT a) without passivation [6] and b) with passivation.

2.1 Simulation Result

Figure 2 shows that the issue of exhibition of a negative conductance at large V_{ds} is caused by the self-heating. Besides, trapping effects take place at the gate/drain surface and in GaN bulk as reported in [6]. Therefore, we deposit Si_3N_4 passivation layer on the top of a HEMT to realize a well-regulated electrical characteristic by separating the top edge of the transistor from chemical reactions that can be in the atmosphere [7].

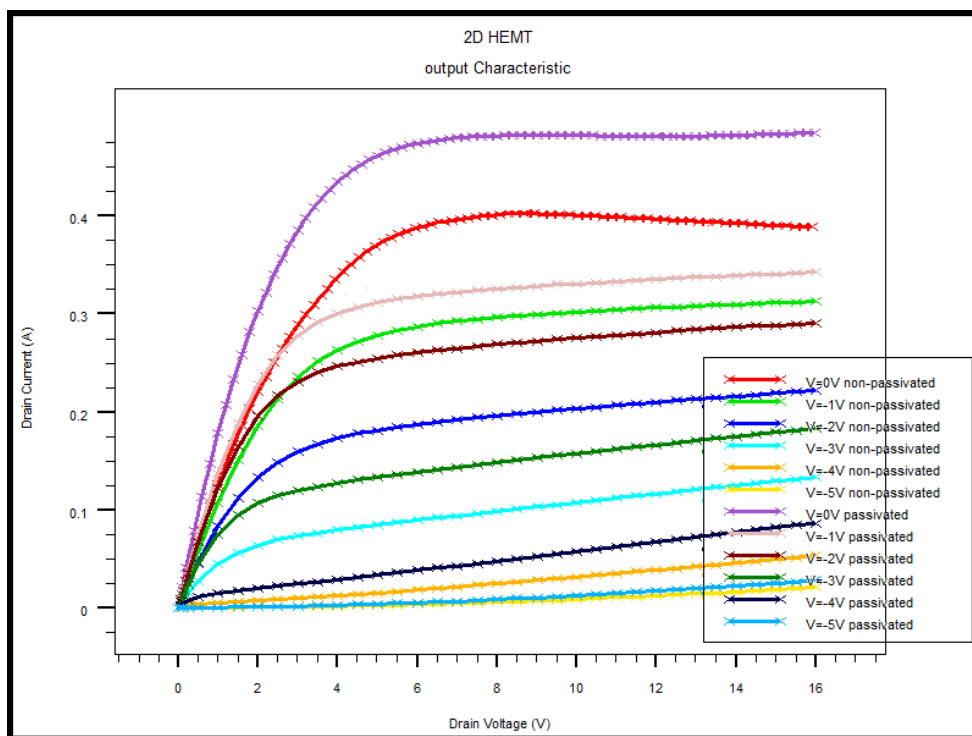


Figure 2. The simulated output characteristic of AlGaN/GaN HEMT a) without passivation [6] and b) with passivation.

In Figure 2, the result of output characteristic exhibits a remarkable increase in drain current and that the maximum current I_{ds} (max) has reached 0.48 A compared with the maximum current

obtained (0.4 A) for the structure in Figure 1(a). The passivation layer prevents the loading of the states on the surface and reduces the trapping mechanism [7]. The increase of the drain current after passivation indicates that the density of the 2D gas increases in turn.

Figure 3 gives the transfer characteristic with and without the passivation layer. A slight decrease in the value of threshold voltage from -3.7 V to -4 V is observed. This is because the passivation layer reduces the surface trap effect. It engenders an increase in the carrier density of 2DEG. Thus, the passivation layer of Si₃N₄ reduces the leakage currents, increases the 2D electron gas density and therefore decreases the voltage of pinch.

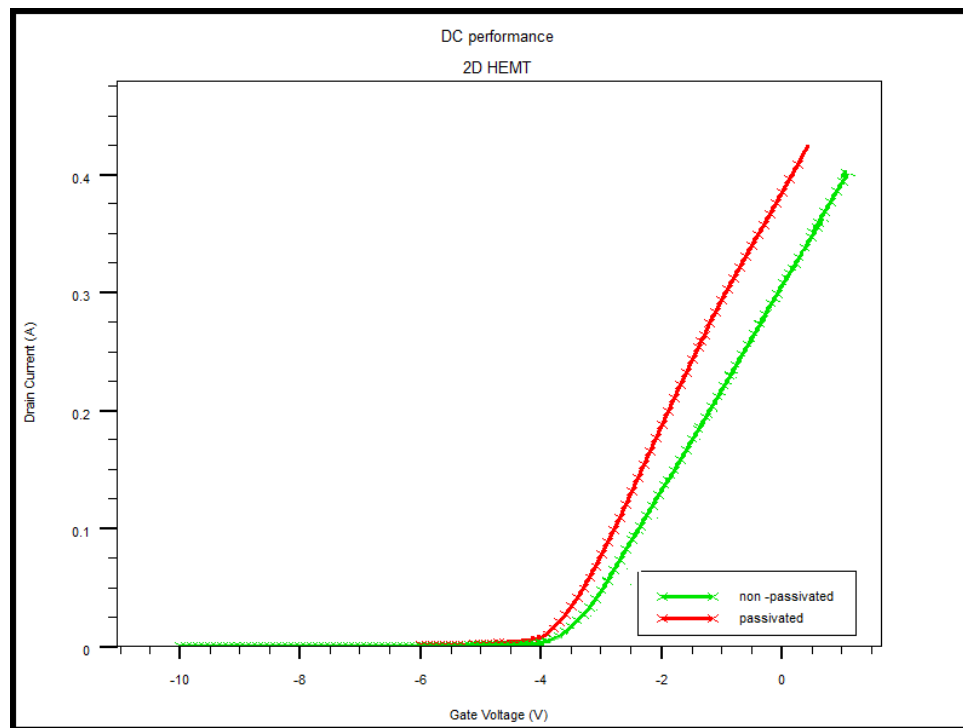


Figure 3. simulated transfer characteristic of AlGaIn/GaN HEMT a) without passivation [6] and b) with passivation.

3. PROPOSED STRUCTURE AND SIMULATION MODEL

In this work, the simulation was performed in 2D by ATLAS of SILVACO TCAD software. This software solves the continuity and Poisson equations with self-coherently at any point of the simulated structure with GUMMEL-NEWTON method. The equations of the different physical models that need to be taken into consideration (mobility models, trap effect, etc.) are solved by relying upon the parameters of materials such as mobility, bandwidth, state densities, etc that were taken from SILVACO ATLAS user's manuals [8].

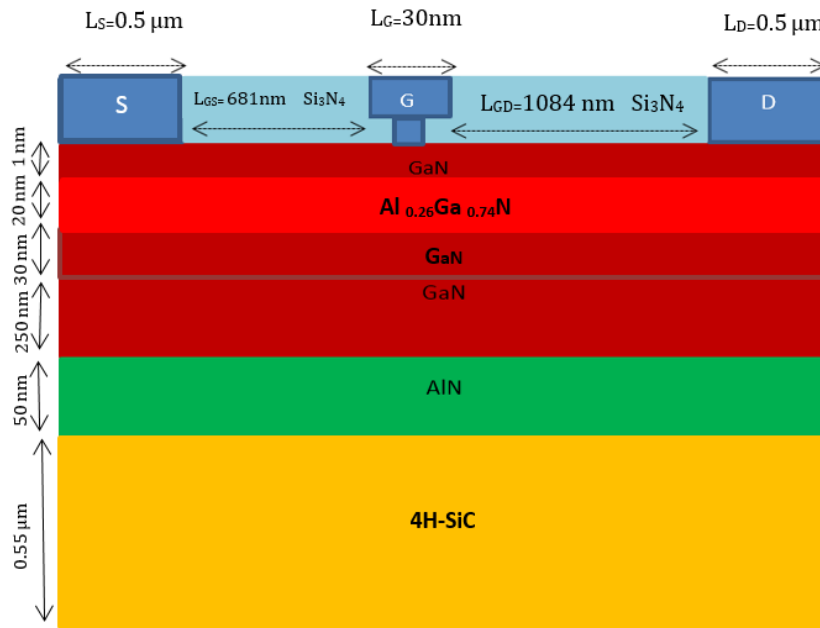


Figure 4. Schematic cross-section of the proposed HEMT.

From the base to the top of the device, we have 0.55 μm of 4H-SiC as substrate, 0.05 μm of nitride aluminium as nucleation layer and 0.25 μm of GaN buffer. 0.03 μm of GaN layer, The channel is 0.2 μm of thick $\text{Al}_{0.26}\text{Ga}_{0.74}\text{N}$ layer and then 1 nm thick n-type GaN cap layer. Finally, 22 nm of the passivation Si_3N_4 layer was added.

The structure has a length of gate $L_G=30$ nm and a stem height of 20 nm. The distances of the source-gate L_{SG} and drain-gate L_{DG} are 681 nm and 1084 nm, respectively. The length of source L_S and drain L_D are 0.5 μm . Several parameters are summarized in Table 1.

Table 1 Device structure parameters

Parameter	Value
Gate length (L_G)	30 nm
Source length (L_S)	0.5 μm
Channel Length	3 μm
GaN channel n^+ doping concentration	3×10^{17} per cm^3
GaN Cap n^+ doping concentration	1×10^{22} per cm^3

First, the basic parameters lattice constant, electron affinity, permittivity and density of states masses should be calculated and introduced, the lattice constant “a” of AlGa_xN can be calculated by linear interpolation:

$$a(\text{Al}_x\text{Ga}_{1-x}\text{N}) = xa(\text{AlN}) + (1 - x)a(\text{GaN}) \quad (1)$$

with $a(\text{AlN}) = 0.3112$ nm, and $a(\text{GaN}) = 0.3189$ nm.

The band-gap of AlGa_xN is calculated from [4][5]:

$$E_G(\text{Al}_x\text{Ga}_{1-x}\text{N}) = xE_G(\text{AlN}) + (1 - x)E_G(\text{GaN}) - 1.3x(1 - x) \quad (2)$$

With $E_G(\text{GaN}) = 3.415$ eV, and $E_G(\text{AlN}) = 6.15$ eV [6].

The electron affinity is given by [7]:

$$\frac{\Delta E_c}{\Delta E_v} = \frac{0.7}{0.3} \tag{3}$$

From this relation, we can calculate the electron affinity accordingly to composition fraction x:

$$\chi(\text{Al}_x\text{Ga}_{1-x}\text{N}) = \chi(\text{GaN}) - 1.89x + 0.91x(1-x) \tag{4}$$

The permittivity as a function of composition fraction x is given by [8]:

$$\varepsilon(\text{Al}_x\text{Ga}_{1-x}\text{N}) = 8.5x + 0.89(1-x) \tag{5}$$

The nitride density of states masses is given by linear interpolations of the values for the binary compounds [9]:

$$m_e(\text{Al}_x\text{Ga}_{1-x}\text{N}) = 0.314x + 0.2(1-x) \tag{6}$$

$$m_h(\text{Al}_x\text{Ga}_{1-x}\text{N}) = 0.417x + 1.0(1-x) \tag{7}$$

Table 2 Physical parameters used in the simulation

Parameter	GaN	AlN	Al _{0.26} Ga _{0.74} N	4H-SiC
E _G (eV)	3.43	6.13	3.88	3.36
χ(cm ² /vs)	4.1	2.2	3.78	3.24
N _c (cm ⁻³)	2.24 10 ¹⁸	4.41 10 ¹⁸	2.75 10 ¹⁸	1.2310 ¹⁹
N _v (cm ⁻³)	2.5 10 ¹⁹	6.75 10 ¹⁸	1.95 10 ¹⁹	4.5810 ¹⁸
ε	8.9	8.5	8.79	6.63

4. RESULTS AND DISCUSSIONS

Figure 5 shows the output characteristic: the drain current (*I_{ds}*) versus drain voltage (*V_{ds}*) for different gate-source voltage. The drain-source bias shifted from 0 V to 15 V and whilst the gate voltage was swept from 0 V to -4 V. The maximum drain current obtained is 600 mA/mm. *R_{ON}* extracted for 0 < *V_{gs}* < 2 V is equal to 0.15 Ω·mm.

The drain-source current (*I_{ds}*) decreases as the gate-source control voltage decreases. When the control voltage becomes more and more negative, the position of the Fermi level moves downwards with respect to the energies in the channel causing a decrease of the drain-source current. Due to the decrease of the charge density in the canal, the obtained results are better than the ones obtained by [6].

Figure 6 shows the transfer characteristic (the drain-source current (*I_{ds}*) versus gate-source voltage (*V_{gs}*) while drain voltage fixed at 0 V. The threshold voltage is -3.5 V, which presents a low threshold voltage thus a good control of the channel and better than was presented by the work [10].

Figure 7 presents the crucial parameter of HEMT, transconductance, which expresses the variation of the drain-source current with respect to the variation of the gate-source voltage, for a constant drain-source voltage. This simulation is performed for a gate-source voltage that varies from 0.0 to -10 V and a drain-source voltage set to 0 V. The simulation indicates a maximum transconductance of 200 mS/mm. The proposed device properties are higher than the values previously reported for similar structures based on AlGa_n/Ga_n heterostructures [10].

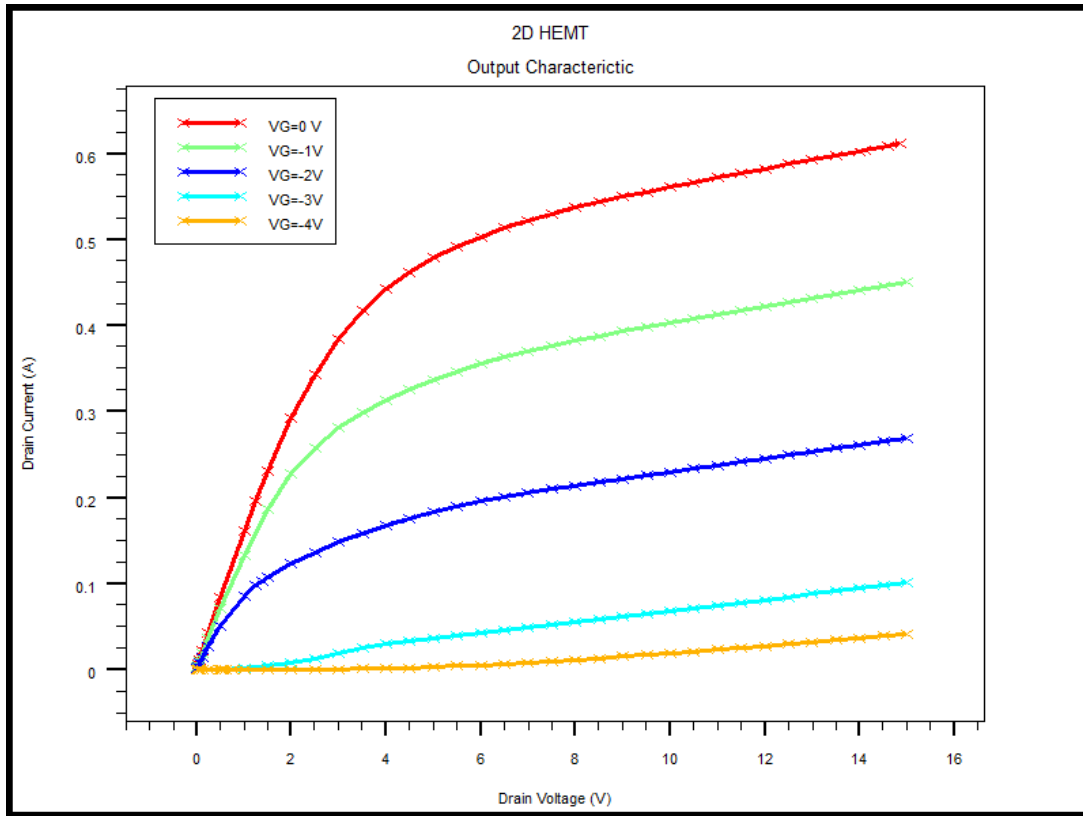


Figure 5. Drain-source current as a function of drain-source voltage.

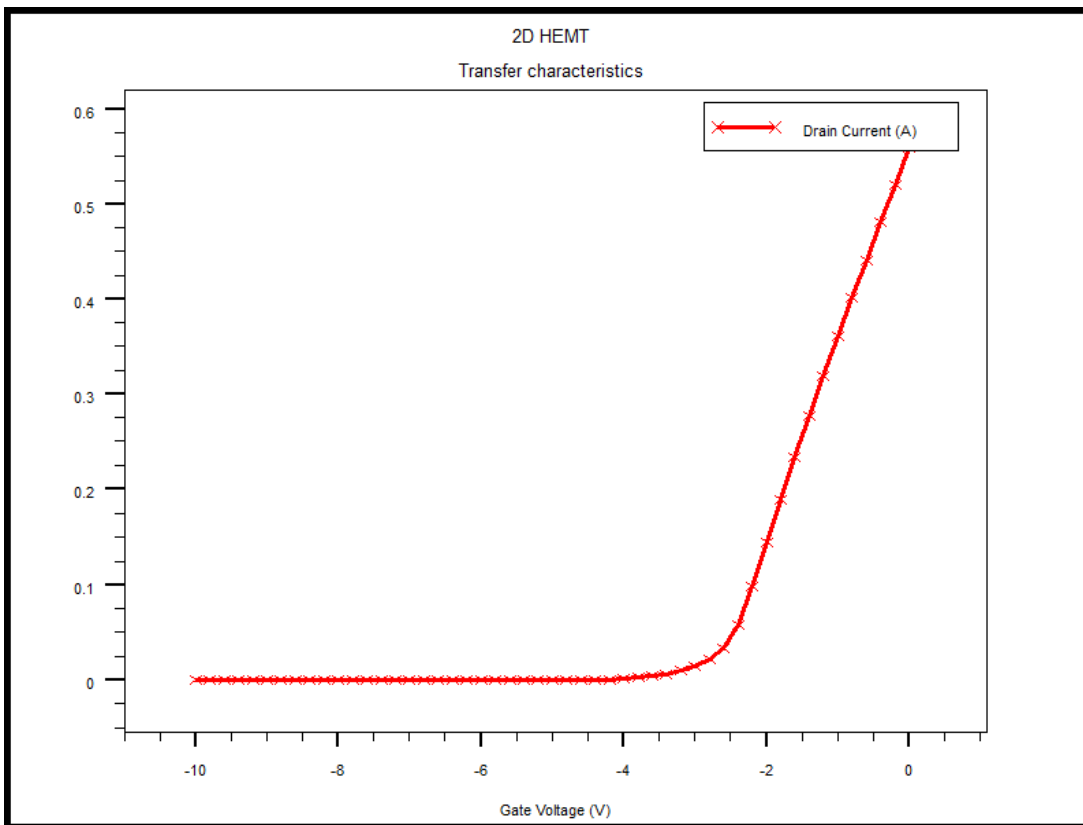


Figure 6. Drain-source current as a function of gate-source voltage.

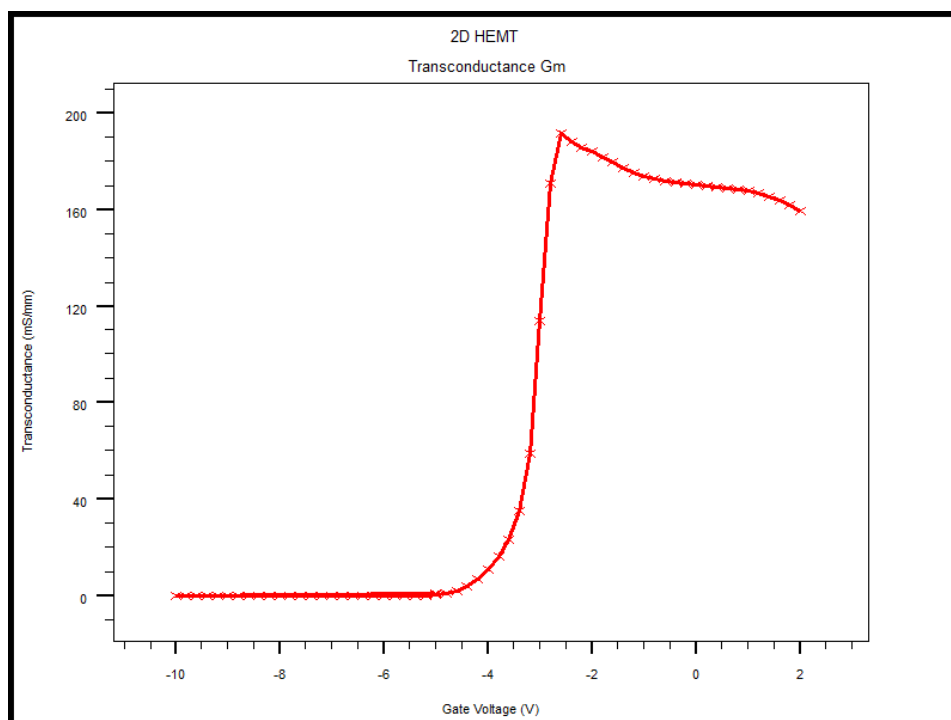


Figure 7. Transconductance versus the gate-source voltage while drain-source bias is fixed at 0 V.

The current gain and unilateral power gain for $V_{ds}=10$ V and $V_{gs}=0$ V are presented in Figure 8. The maximum gain current is 190 dB while the unilateral power gain is 164 dB. The proposed device presents a cutoff frequency of 50 GHz and a maximum frequency of 150 GHz indicating that the obtained result is excellent compared to the value reached in state of art for such structures. Hence, the proposed device is a good candidate for microwave and power application.

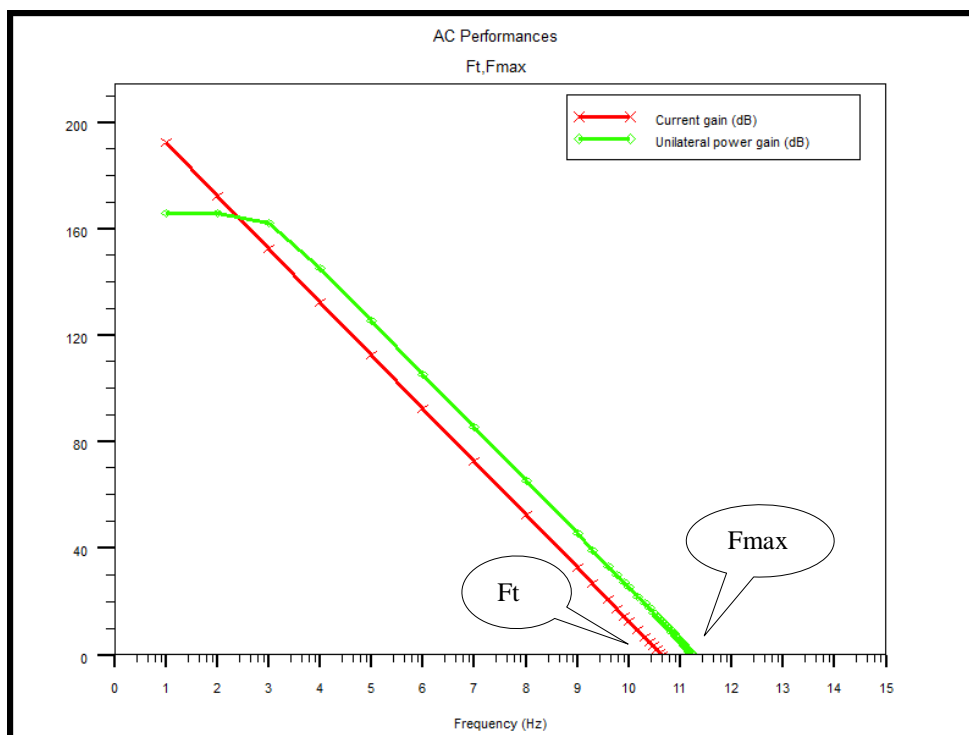


Figure 8. Gains current gain and unilateral power gain versus frequency $V_{ds}=10$ V and $V_{gs}=0$ V.

Figure 9 presents the stable maximum power gain (Gms) and available maximum power gain (Gma). The peak value of Gma and Gms are obtained at 110 dB which stand for a suitable stability performance for microwave and low-noise amplifier applications.

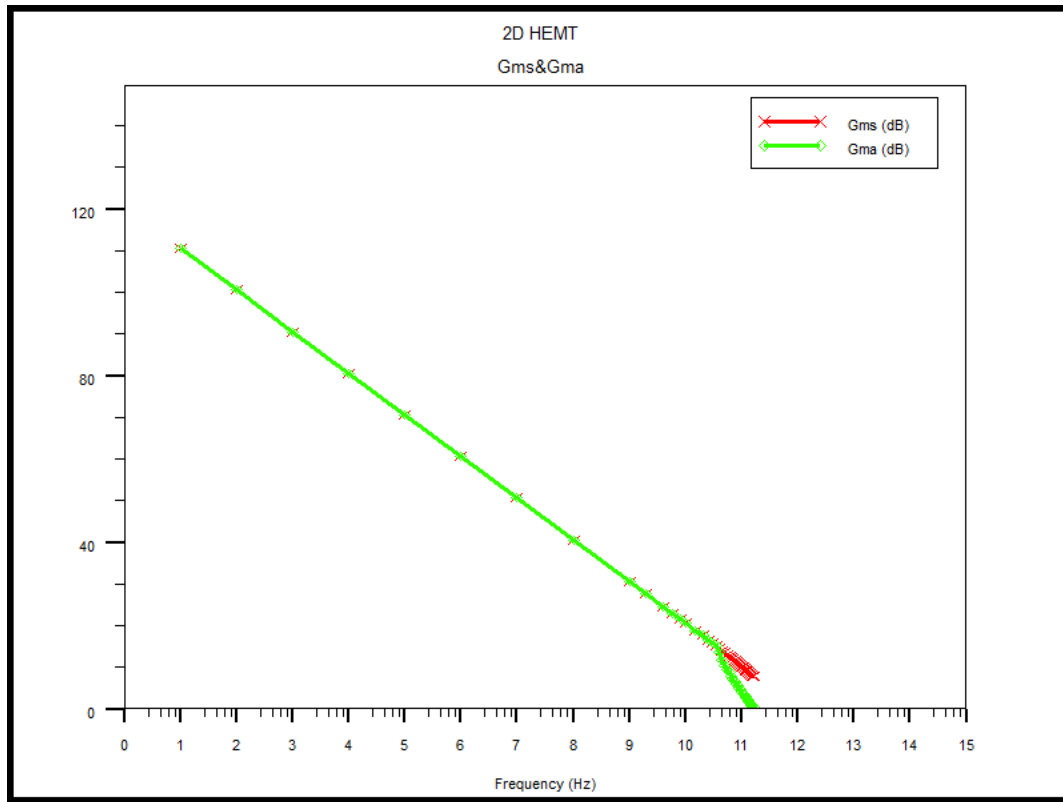


Figure 9. Stable maximum power gain (GMS) and available maximum power gain (GMA) at $V_{ds}=10$ V and $V_{gs}=0$ V.

Figure 10 shows the Sub-threshold Swing (SS) slope which is determined from the $\log(I_{ds})$ characteristic as a function of V_{gs} . It corresponds to the gate-source voltage to be applied to reduce the drain current. It is obtained for V_{gs} values close to the pinch at $V_{ds}=0$ V.

The SS is calculated by the following equation:

$$SS = \frac{\Delta V_{gs}}{\Delta \log(I_{ds})} \tag{9}$$

$$SS = (V_{gs2} - V_{gs1}) / \text{dec}$$

$$SS = [-3.8 - (-4)] \text{ V / dec}$$

$$SS = 0.2 \text{ V / dec}$$

The simulated device offers slope under the threshold (SS) about 200 mV/Dec. This is a crucial factor for component quality and power consumption in static and back-up power applications. It is a very interesting value compared to the results found in the work [10].

The I_{on}/I_{off} ratio is about 10^9 higher than the ratio calculated in [14]. A high value of I_{on}/I_{off} ratio is a major parameter for power application. Moreover, this parameter is attractive to power consumption in static and standby power applications.

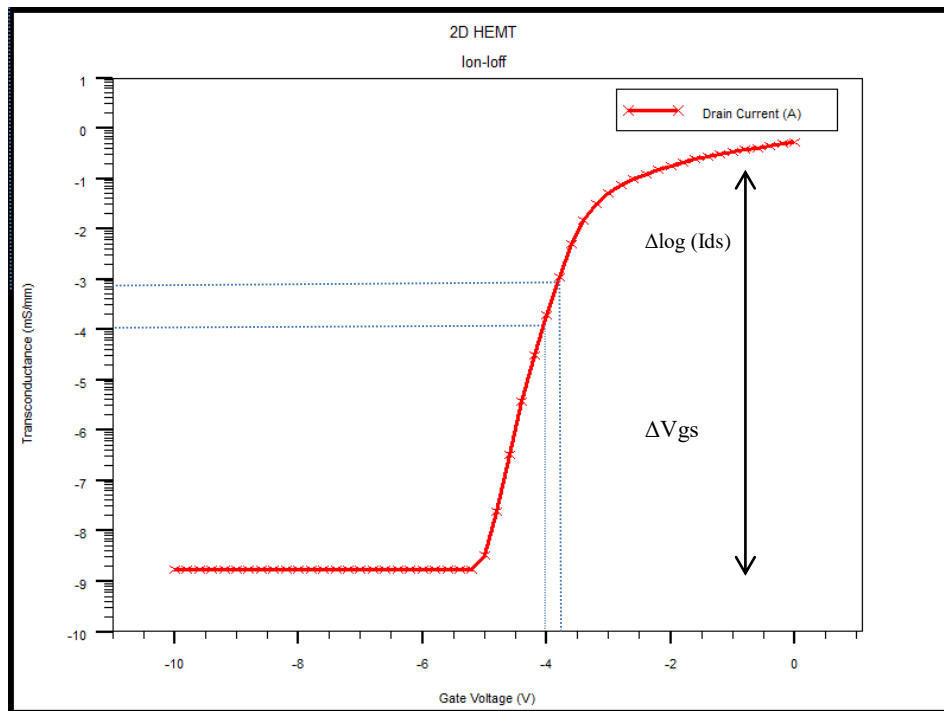


Figure 10. Drain current plotted with a log scale as a function of gate-source voltage.

The drain induced barrier lowering (DIBL) is the most important phenomenon for high drain voltages in short channel transistors and is mainly used for digital applications. In this work, the DIBL is calculated for the two threshold voltages V_{th1} and V_{th2} which respectively correspond to the following drain-source voltages V_{ds1} and V_{ds2} . The DIBL is calculated by the following equation:

$$DIBL = \text{Abs} [\Delta V_{th} / \Delta V_{ds}] \quad (10)$$

$$DIBL = \text{Abs} [(V_{th2} - V_{th1}) / (V_{ds2} - V_{ds1})]$$

$$\text{For } V_{ds1} = 0.5 \text{ V and } V_{ds2} = 5$$

$$DIBL = 22 \text{ mV} / \text{V}$$

The obtained value of DIBL is a good value compared to the results found in the literature, at room temperature.

Table 3 summarizes a comparison of the main performances (maximum drain current, threshold voltage, transconductance subthreshold slope and cut-off frequency) calculated in this work versus the result obtained by [15], [16], [13] and [6].

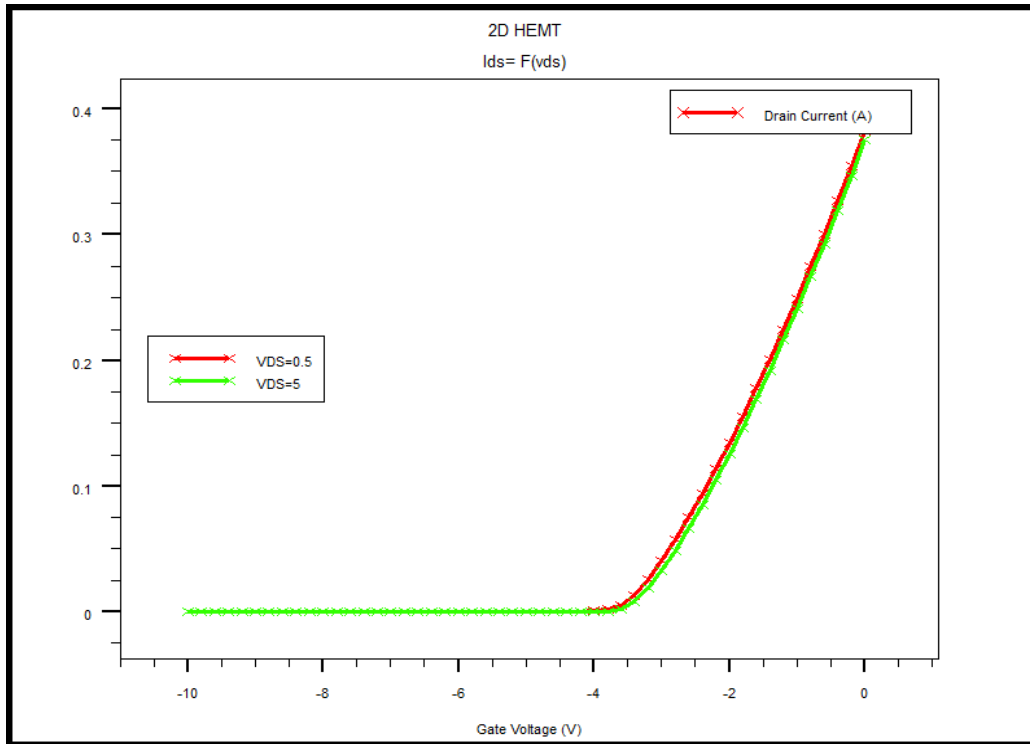


Figure 11. The drain-source current (I_{ds}) as a function of gate-source voltage (V_{gs}) while the drain voltage is fixed at 0.5 V, 5.0 V and $V_{gs}=-1$.

Table 3 Comparison of the performances of the proposed structure versus references [15] [16] [13] [6]

	[15]	[16]	[13]	[6]	This work
Maximum Drain Current (mA)	15	658	580	400	600
Threshold Voltage (V)	-5.9V	-5.5V	-4V	-3.7	-3.5
Transconductance (ms)	260	123	122.5	--	200
Subthreshold Slope (V/dec)	0.220	--	0.185	--	0.2
f_T (GHZ)	63 GHz	2.6 GHZ	73.6 GHz	19 GHZ	50 GHz

5. CONCLUSION

To sum up, this paper has discussed the DC and AC performances of HEMT based on AlGaN/GaN by using two-dimensional TCAD simulator (SILVACO TCAD). The better channel control with T shape gate has been achieved by suppressing the undesirable effect such as short channel effect (SCE) in terms of DIBL and SS. The device demonstrates a maximum drain current of 600 A/mm, a threshold voltage of -3.5 V, a maximum transconductance of 200 mS/mm, an I_{on}/I_{off} ratio of 109, DIBL of 22 mV/V, and SS of 200 mV/dec. Otherwise, a considerable AC performance in terms of cut-off frequency (f_t) and maximum oscillation frequency (F_{max}) has been attained. A comparison study was conveyed out with a recent state of the art and the obtained results contribute as reference for future research for power and high frequencies applications.

REFERENCES

- [1] W. L. S. Sinha, "SiGe-based Re-engineering of Electronic Warfare Subsystems," Switzerland: Springer International Publishing **329** (2017) 307.
- [2] M. M. Meneghesso, Gaudenzio, "Power GaN Devices", Switzerland: Springer International Publishing **380** (2017) 2.
- [3] D. B. Subhra Chowdhury, "Effect of device parameters on transmission coefficient of Al_{0.2}Ga_{0.8}N/GaN Resonant Tuning Diode grown on silicon substrate," *Nanoelectronics and Materials*, **6** (2013) 129-137.
- [4] Gassoumi *et al.*, "Improvement of DC and RF Performances of an AlGa_{0.99}N Back-Barrier Simulation Study," in the 9th international symposium on advanced topics in electrical engineering, Bucharest, Romania, (2015).
- [5] F. Jabli, M. A. Zaidi, N. Ben Hamadi, S. Althoyaib, M. Gassoumi, "Characterisation of the effect of surface passivation with SiO₂/SiN on deep levels in AlGa_{0.99}N/GaN/Si HEMTs," *Journal of Alloys and Compounds* **653** (2015) 624–628.
- [6] M. Gassoumi, A. Helali, M. Gassoumi, C. Gaquiére & H. Maaref, "DC and RF characteristic of high-electron-mobility transistor (HEMT) on AlGa_{0.99}N/GaN/Si for power applications," *Journal of Ovonic Research* **13**, 04 (July - August 2017) 211 - 217.
- [7] A. S. Augustine Fletcher, D. Nirmal, "A Survey of Gallium Nitrate HEMT for RF and High Power application," *Superlattices and Microstructures* **38** (2017) 2-3.
- [8] ATLAS user's manual www.silvaco.com, chapter 2: defining material parameters, models and choosing numerical methods, (2004) 27-38.
- [9] O. Ambacher, J. A. Majewski, C. Miskys, A. Link, M. Hermann, M. Eickhoff, M. Stutzmann, F. Bernardini, V. Fiorentini, V. Tilak, B. Schaff, & L. F. Eastman, "Pyroelectric properties of Al (In)Ga_{0.99}N/GaN hetero- and quantum well structures," *J. Phys.: Condens. Matter* **14**, 3399 (2002).
- [10] J. Piprek, D. Lasasosa, D. Pasquariello, & J. E. Bowers "Physics of waveguide photodetectors with integrated amplification", *Proc. SPIE 4986, Physics and Simulation of Optoelectronic Devices XI*, (25 July 2003).
- [11] O. Ambacher, B. Foutz, J. Smart, J. R. Shealy, N. G. Weimann, K. Chu, M. Murphy, A. J. Sierakowski, W. J. Schaff, & L. F. Eastman, "Two-dimensional electron gases induced by spontaneous and piezoelectric polarization in undoped and doped AlGa_{0.99}N/GaN heterostructures," *Appl. Phys* **334**, 87 (2000).
- [12] J. M. R. I. Vurgaftman, "Band parameters for III–V compound semiconductors and their alloys," *Applied Physics* **5815** (2001) 89.
- [13] S. Chatterjee, "Analysis of AlGa_{0.99}N/GaN High Electron Mobility Transistor for High Frequency Application," in *Proc. Int. conf. Devices for Integrated Circuit (DevIC)*, Kalyani, India, IEEE Xplore, (2017).
- [14] P. Murugapandiyar, S. Ravimaran, J. William, "DC and microwave characteristics of AlN spacer based Al_{0.37}Ga_{0.63}N/GaN HEMT on SiC substrates for high power RF applications," *Int. J. Nanoelectronics and Materials* **10** (2017) 111-122.
- [15] T. De. Mohapatra, A. K. Panda, "DC and RF Performance Analysis of AlGa_{0.99}N/GaN based HEMT," in *IEEE 2nd International Conference on Communication, Control and Intelligent Systems (CCIS)* IEEE Xplore, (2016) 182-183.
- [16] Y. Murase, K. Asano, I. Takenaka, Y. Ando, H. Takahashi & C. Sasaoka, "T-Shaped Gate GaN HFETs on Si With Improved Breakdown Voltage and f_{max}," *IEEE Electron Device Letters* **35**, 5 (May 2014), 524-526.